The Deflection Control of a Thin Cantilever Beam by Using a Piezoelectric Actuator / Sensor

Waleed Khalid. Al-Ashtari
Mech. Eng. Dept. College of Engineering University of Baghdad
e-mail: waleedalashtari@yahoo.com

Abstract

In this research, the governing equation of the thin smart beam transverse deflection was derived by the same procedure that the Bernoulli-Euler equation derived but with some additional mathematical terms to be valid for describing the smart beam. The engineering control techniques were used to obtain the solution of the proposed differential equation for the smart cantilever beam where with some auxiliary equations and modifications a block diagram for any type of applied load (static, or cyclic) as the input and the beam deflection as the output was constructed. For insuring an efficient reduction in the beam deflection an integrated system with a voltage amplifier and lead controller was designed. Many cases were studied and simulated including the variation of load nature, and the number of collocated piezoelectric actuator/sensor pairs and in all cases a valuable deflection reductions were obtained.

Keywords: *Smart Beam, Ordinary Beam, Bernoulli-Euler Equation, Voltage Amplifier, and Lead Network Controller.*

1. Introduction

Piezoelectric transducers have become increasingly popular in vibration control applications. They are used as sensors and as actuators in structural vibration control systems. They provide excellent actuation and sensing capabilities. The ability of piezoelectric materials to transform mechanical energy into electrical energy and vice versa was discovered over a century ago by Pierre and Jacque Curie. These French scientists discovered a class of materials that when pressured, generate electrical charge, and when placed inside an electric field, strain mechanically.

Piezoelectricity, which literally means "electricity generated from pressure" is found naturally in many monocrystalline materials, such as quartz, tourmaline, topaz and Rochelle salt. However, these materials are generally not suitable as actuators for vibration control applications. Instead, man-made polycrystalline ceramic materials, such as lead zirconate titanate (PZT), can be processed to exhibit significant piezoelectric properties. PZT ceramics are relatively easy to produce, and exhibit strong coupling between mechanical and electrical domains. This enables them to produce comparatively large forces or displacements from relatively small applied voltages, or vice versa. Consequently, they are the most widely utilized material in manufacturing of piezoelectric transducers.

Piezoelectric transducers are available in many forms and shapes. The most widely used piezoelectric transducers are in the form of thin sheets that can be bonded to or embedded in composite structures. As actuators they are mainly used to generate moment in flexible structures, while as sensors they are used to measure strain.

Piezoelectric transducers are used in many applications such as structural vibration control, precision positioning, aerospace systems, and more recently they have been critical in advancing researches in nanotechnology [13].

To this end, many researchers have concentrated on dynamic modeling of piezoelectric materials as elements of intelligent (smart) structures [5, 6, 10, 19, 23] while a number of others have focused on control methods of piezoelectric actuators for suppressing vibrations and noise reduction [2, 8, 20]. [21] Conducted studies on the application of segmented piezoelectric transducers PZT ceramics and poly vinylidene fluoride (PVDF) materials for this purpose, [4] investigated active vibration control by utilizing hybrid smart actuators constructed from PZT and shape memory alloy. [18] Studied stability issues in controlling a flexible beam. A quite comprehensive literature review has been given in [19].In selecting a PZT actuator for vibration control; it is useful to know how the physical parameters of a PZT can affect system performance. This issue is of paramount importance if one notes that a PZT actuator has the major drawback of limited capability to produce high torques. This fact reduces the effectiveness of the PZT usage for suppressing vibrations. There are two ways to remedy this problem. One of these calls for the use of stronger PZT actuators such as the one developed at NASA's Langley research center for alleviating the buffet load in the tail fin of the fuselage [16].The other solution involves finding optimum values of the physical parameters to make use of the maximum strength of the actuator. Previous work has tried to address this issue, in an attempt to obtain the optimum size and location of the actuator [12, 15]. [9] Proposed a measure of modal controllability based on the angle between the normalized left eigenvectors of the system and the control input matrix. [11] Presented a modal cost to rank each mode's participation in system output. [1] Reported a weighted controllability measure

by modifying Hamdan's controllability index. They also considered a penalty for the length of the actuator in formulating the optimization problem. [24] Defined a participation factor to address the participation of a mode in a state, specified as output. [14] Introduced the idea of spatial controllability in order to include the effect of actuator location in the optimization problem. [25] Considered the effect of the adding an actuator/sensor on the mass and stiffness of the structure and combined that with the control performance index to obtain the optimum values for the location, size and feedback gains, simultaneously. However, a clear description of the actuator performance with respect to each individual mode of vibration needs to be given more attention. The degree by which a certain parameter can affect each resonance mode motivates further investigations. The use of the controllability Grammian and singular value decomposition of the system dynamics can provide practical guidelines for selecting the optimal values of the aforementioned parameters. [22] Introduce an analysis and comparison of the classical and optimal feedback control strategies on the active control of vibrations of smart piezoelectric beams. [3] They developed a simplified and consistent theory to actively control sandwich beams (the upper and bottom surfaces are covered entirely with a piezoelectric layer) at small and large amplitude.

In this research, the term smart beam will refer to a beam with a finite number of collocated piezoelectric actuator/sensor pairs, while ordinary beam will refer simply to the beam itself without any actuators or sensors. A smart beam differential equation had been derived by the same procedure that the Bernoulli-Euler equation derived with some mathematical modifications to be applicable for the smart beam actuating by any type of applied load such as static or cyclic. The engineering control techniques was used to obtain the solution of proposed differential equation where with some auxiliary equations and modifications a block diagram as the applied load be the input and as the smart beam deflection be the output was constructed as will be shown later. Also in this research, a beam deflection reduction system with a lead network controller and a high voltage amplifier has been designed mainly for two reasons: the first was to amplify the voltage generated by the sensor to be able to handle and transmit it efficiently to the actuator. And the second was to enhance the system response.

2. The Thin Smart Beams Governing Equation

Now, the derivation of the smart beam differential equation actuated by an external load (static or cyclic) will be accomplished. Let us consider a setup as shown in Fig.1, where m of identical collocated piezoelectric actuator/sensor pairs are bonded to a beam. The assumption that all piezoelectric transducers are identical is only adopted to simplify the derivations, and can be removed if necessary. The ith actuator is exposed to a voltage of $e_{ai}(t)$ and the voltage induced in the ith sensor is $e_{si}(t)$. the beam has a length of l_b, width of w_b, and thickness of t_b Corresponding dimensions of each piezoelectric transducer are l_p, w_p, and t_p. Furthermore, the transverse deflection of the beam at point x and time t is denoted by v(x, t).

It is well known that Bernoulli-Euler equation governs the transverse vibration of beams. Therefore, the derivation of the smart beam equation will follow the same procedure that used in derivation of Bernoulli-Euler equation but with changing the applying load condition.

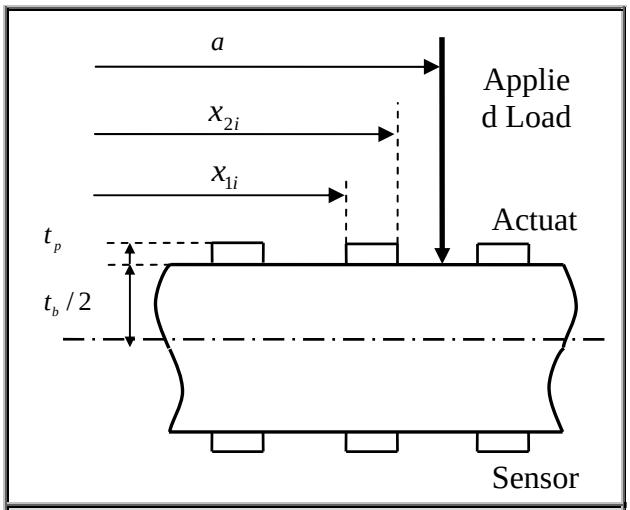

Figure (1) A Beam with A Finite Number of Collocated Piezoelectric Actuator/Sensor Pairs and Applied Load

Consider a beam in bending, in the x-y plane, with x as the longitudinal axis and y as the transverse axis, of bending deflection, as shown in Fig.2. The required equation is developed by considering the bending moment – deflection relation, rotational equilibrium, and transverse dynamics of a smart beam element.

2.1. Rotatory Dynamics

Consider the beam element δx, as shown in Fig.2, where forces and moments acting on the element are indicated.

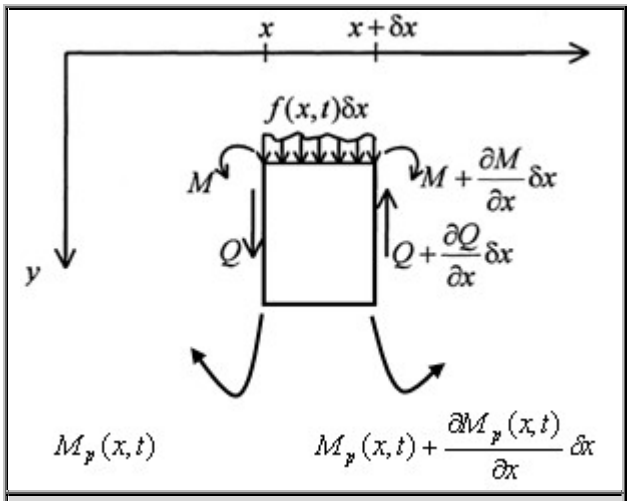

Figure (2) Dynamic of a Beam Element in Bending

Here, $f(x,t)$ is the excitation force per unit length acting on the beam in the transverse direction at location x, and $M_p(x,t)$ is the total moment that generated by all the actuators, which act oppositely to the applied load and can expressed by

$$M_p(x,t) = \sum_{i=1}^{m} M_{pi}(x,t) \qquad (1)$$

Where m is the number of identical collocated piezoelectric actuator / sensor pairs which are bounded to the beam. The equation of the angular motion is given by the equilibrium condition of moments:

$$M - M_p(x,t) + Q\delta x - \left(M + \frac{\partial M}{\partial x}\partial x\right) + \left(M_p(x,t) + \frac{\partial M_p(x,t)}{\partial x}\partial x\right) = 0 \qquad (2)$$

where the moment deflection relation can expressed as

$$M = E_b I_b \frac{\partial^2 v}{\partial x^2} \qquad (3)$$

simplifying Eq.2 and substituting Eq.3 into it will give

$$Q = \frac{\partial}{\partial x}\left(E_b I_b \frac{\partial^2 v}{\partial x^2}\right) - \frac{\partial M_p(x,t)}{\partial x} \qquad (4)$$

2.2 Transverse Dynamics

The equation of transverse motion for element δx is

$$(\rho_b A_b \delta x)\frac{\partial^2 v}{\partial t^2} = f(x,t)\delta x + Q - \left(Q + \frac{\delta Q}{\partial x}\delta x\right) \qquad (5)$$

Here, ρ_b is the mass density of the beam material, more simplifying will give

$$\rho_b A_b \frac{\partial^2 v}{\partial t^2} + \frac{\partial Q}{\partial x} = f(x,t) \qquad (6)$$

Now, substituting Eq.4 into Eq.6, will give the governing equation of forced transverse vibration of smart beam with finite number of actuators

$$\rho_b A_b \frac{\partial^2 v}{\partial t^2} + \frac{\partial^2}{\partial x^2}\left(E_b I_b \frac{\partial^2 v}{\partial x^2}\right) = \frac{\partial^2 M_p(x,t)}{\partial x^2} + f(x,t) \qquad (7)$$

3. The Engineering Control Solution

Now, Eq.7 will be solved by using the engineering control techniques such as a differential equation linearization and system block diagram construction, but this deferential equation must be linearized to be able for handling it and this done firstly by specifying the case of study where a cantilever beam has been chosen, and follow the below procedure

3.1 Beam and Actuator Equation

If young's modules and second moment of area about the neutral axis are constant then

$$\rho_b A_b \frac{\partial^2 v}{\partial t^2} + E_b I_b \frac{\partial^4 v}{\partial x^4} = \frac{\partial^2 M_p(x,t)}{\partial x^2} + f(x,t) \qquad (8)$$

As shown in Fig.1 where the actuating force is applied at $x = a$, then by using Dirac delta Eq.8 can be rewrite as

$$\rho_b A_b \frac{\partial^2 v}{\partial t^2} + E_b I_b \frac{\partial^4 v}{\partial x^4} = \frac{\partial^2 M_p(x,t)}{\partial x^2} + f(t)\,\delta(x-a) \qquad (9)$$

And the moment exerted on the beam by the ith actuator can expressed [13] as

$$M_{pi}(x,t) = \bar{k}\, e_{ai}(t)\left[u(x - x_{1i}) - u(x - x_{2i})\right] \qquad (10)$$

where $u(x)$ is a unit step input and $\bar{k}$ was formulated by [26] as

$$\bar{k} = \frac{E_b E_p t_b^2 w_b w_p d_{31}}{E_b t_b w_b + E_p t_p w_p} \quad (11)$$

Substitute that

$$v(x,t) = \sum_{k=1}^{\infty} Y_k(x) q_k(t) \quad (12)$$

where normalized mode shapes for the cantilever beam are [7]

$$Y_k(x) = \sin\lambda_k x - \sinh\lambda_k x + \alpha_k\left[-\cos\lambda_k x + \cosh\lambda_k x\right] \quad (13)$$

where

$$\alpha_k = \frac{\sinh\lambda_k l_b + \sin\lambda_k l_b}{\cosh\lambda_k l_b + \cos\lambda_k l_b} \quad (14)$$

and $k = 1, 2, 3, \cdots$

after the derivation, the following equation must be satisfied for cantilever beam case [7]

$$\cos\lambda_j l_b + \cosh\lambda_j l_b = -1 \quad (15)$$

multiply Eq.9 by $Y_j(x)$; integrate over $x = [0, l_b]$ and use the orthogonality of mode shapes to obtain

$$E_b I_b \lambda_j^4 \frac{l_b}{2} q_j(t) + \rho_b A_b \frac{l_b}{2} \ddot{q}_j = \bar{k}\,\psi_{ji}\, e_{ai}(t) + f(t)\left(\sin\lambda_j a - \sinh\lambda_j a + \alpha_j\left[-\cos\lambda_j a + \cosh\lambda_j a\right]\right) \quad (16)$$

where

$$\psi_{ji} = \int_0^l Y_j(x)\left[\delta'(x - x_{1i}) - \delta'(x - x_{2i})\right]dx \quad (17)$$

and using the derivative Dirac delta function property stated in [13], will give

$$\psi_{ji} = Y_j'(x_{2i}) - Y_j'(x_{1i}) \quad (18)$$

now Eq.16 can be rewrite as

$$\ddot{q}_j + \omega_j^2 q_j(t) = \gamma\,\psi_{ji}\, e_{ai}(t) + \beta_j\, f(t) \quad (19)$$

where

$$\omega_j = \lambda_j^2 \sqrt{\frac{E_b I_b}{\rho_b A_b}} \quad (20)$$

$$\beta_j = \frac{2}{\rho_b A_b l_b}\left(\sin\lambda_j a - \sinh\lambda_j a + \alpha_j\left[-\cos\lambda_j a + \cosh\lambda_j a\right]\right) \quad (21)$$

$$\gamma = \frac{2\bar{k}}{\rho_b A_b l_b} \quad (22)$$

To this end we point out that the differential equation Eq.19 dose not contains a term to a count for the natural damping associated with beam. The presence of damping can be incorporated into Eq.19 by adding the term $2\zeta_j\omega_j\dot{q}_j$ to Eq.19. This results in the differential equation

$$\ddot{q}_j + 2\zeta_j\omega_j q_j + \omega_j^2 q_j(t) = \gamma\, e_{ai}(t) + \beta_j\, f(t) \quad (23)$$

Applying the Laplace transform to Eq.23, assuming zero initial conditions and solving for beam deflection and for N mode shapes, will get

$$V(s) = \gamma \sum_{j=1}^{N} \frac{\psi_{ji} Y_j(x)}{s^2 + 2\zeta_j\omega_j s + \omega_j^2} E_{ai}(s) + \sum_{j=1}^{N} \frac{\beta_j Y_j(x)}{s^2 + 2\zeta_j\omega_j s + \omega_j^2} F(s) \quad (24)$$

3.2. Sensor Equation

The voltage generated by the ith piezoelectric sensor e_{si} can be expressed as [13]

$$e_{si}(t) = \frac{d_{31} E_p W_p}{C_p} \int_{x_{1i}}^{x_{2i}} \varepsilon_{si}\, dx \quad (25)$$

The expression of the mechanical strain in sensor patch can be obtained from [13]

$$\varepsilon_{si} = -\left(\frac{t_b}{2} + t_p\right)\frac{\partial^2 v}{\partial x^2} \quad (26)$$

now $e_{si}(t)$ will be

$$e_{si}(t) = -\left[\frac{d_{13} E_p W_p}{C_p}\left(\frac{t_b}{2} + t_p\right) \sum_{j=1}^{N} \frac{\psi_{ji}}{Y_j}\right] v(t) \quad (27)$$

Applying Laplace transform to result equation, assuming zero initial condition we get

$$\frac{E_{si}(s)}{V(s)} = -\frac{d_{13}E_p W_p}{C_p}\left(\frac{t_b}{2}+t_p\right)\sum_{j=1}^{N}\frac{\psi_{ji}}{Y_j} = -\sum_{j=1}^{N}k_{ji} \quad (28)$$

4. Ordinary Thin Beams Transfer Function

Starting from Bernoulli-Euler equation for constant young's modules and second moment of area about the neutral axis and for the actuating force is applied at $x = a$, and following the previous derivation procedure and for N mode shape, will have

$$\frac{V(s)}{F(s)} = \sum_{j=1}^{N}\frac{\beta_j Y_j(x)}{\left[s^2 + 2\zeta_j\omega_j s + \omega_j^2\right]} \quad (29)$$

5. Smart Beams Block Diagram

A complete block diagram representing the smart beam had been constructed, where Form the previous derived equations and with some block diagram modification, the block diagram that shown in Fig.4 had obtained

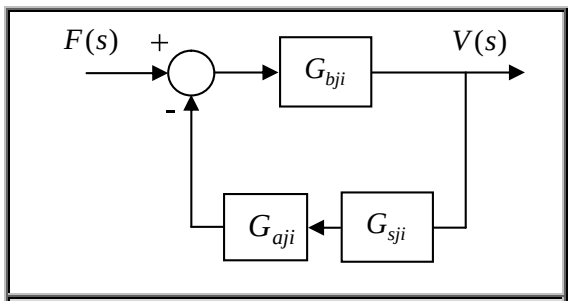

Figure (4) The Block Diagram for Smart Beam with m Collocated Piezoelectric Actuator / Sensor Pairs and N Beam Vibration Mode Shapes

The transfer function matrix G_{bj} shown in Fig.4 consists of a very large number of parallel second order terms while the transfer functions G_{sji} and G_{aji} have a m number of parallel terms, and there values can be expressed as

$$G_{bj} = \sum_{j=1}^{N}\frac{\beta_j Y_j}{s^2 + 2\zeta_j\omega_j s + \omega_j^2} \quad (30)$$

$$G_{sji} = \sum_{i=1}^{m}\sum_{j=1}^{N}k_{ji} \quad (31)$$

$$G_{aji} = \gamma\sum_{i=1}^{m}\sum_{j=1}^{N}\frac{\psi_{ji}}{\beta_j} \quad (32)$$

5. 1 The Proposed Instrumentation

Practically, the voltage generated by the piezoelectric sensor was very small to handle and transmitted to the piezoelectric actuator, therefore, the needs for an integrated instruments system not only for amplifying purpose but also for controlling the beam response. Fig.5 shows the overall proposed system components.

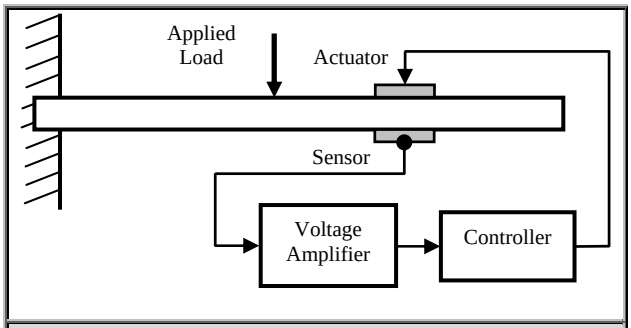

Figure (5) The Proposed Instrumentation

5.2 First Mode Voltage Amplifier

After studying and analyzing the proposed system block diagram shown in Fig.4 and for the first mode shape case the voltage amplifier gain for the ith collocated piezoelectric actuator / sensor pair was formulated to be

$$K_a = \frac{\omega_1^2 + Y_1 k_{1i}\psi_{1i}}{\beta_1 Y_1} \quad (33)$$

5.3 First Mode Controller Design

In most scenarios, only control of a limited bandwidth is of importance. Typically N modes of the structure would fit within this bandwidth while modes N + 1 and above are left uncontrolled. The uncontrolled modes, however, do exist and have the potential to destabilize the closed-loop system. Therefore, the existence of these modes should be taken into account, and a controller should be designed to ensure adequate damping performance, as well as stability in the presence of these out-of-bandwidth modes.

In this work, a first mode controller had been designed and the needs for λ_1 is essential and it can be found from Eq.15 where its first root is

$$\lambda_1 l_b = 1.875 \quad (34)$$

The lead controller shown in Fig.6 had been chosen because of its unique properties especially its property to accelerate the system response. For performing the controller design some physical properties for the desired system response must be assumed in order to be achieved by the controller operation.

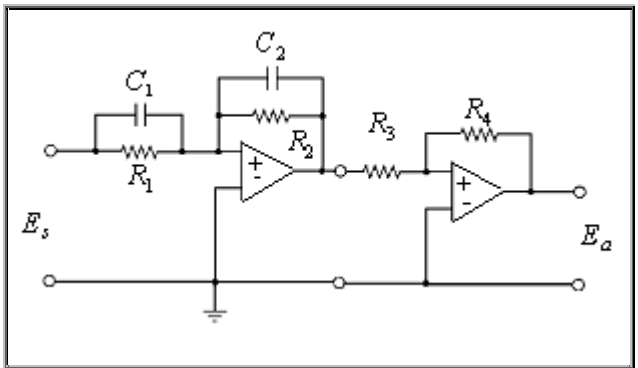

Figure (6) Electronic Circuit of A Lead Network

The transfer function of the lead network compensator can be expressed as [17]

$$G_c = K_c \alpha \frac{Ts+1}{\alpha Ts+1} \quad \textbf{35}$$

Referring to Fig.6,

$$T = R_1C_1,\ \alpha T = R_2C_2,\ K_c = \frac{R_4C_1}{R_3C_2}$$

, and $\alpha = \frac{R_2C_2}{R_1C_1}$

Executing the control system design by frequency response method based on Bode plot as stated by [17], where the assumptions are the static velocity error about $20\,s^{-1}$ and the phase margin at least 50°. After accomplishing the design calculations the following controller transfer function had obtained

$$G_c = \frac{0.79(s+23.43)}{(s+33.47)} \quad \textbf{36}$$

Where $K_c = 0.79$, $\alpha = 0.7$, and $T = 0.043$.

6. Results And Discussion

SIMULINK / MATLAB software was constructed to simulate the proposed system block diagram. The properties that listed in Table 1 which was adopted from [13] had been used as numerical values for such software.

It was decided that the results figures exhibited for a very short time about 1000 ms, to show clearly the beam transient response and the controller effect.

The simulation results of the ordinary beams are showing the high accuracy of the ordinary beam transfer function in comparing with the analytical solution given by any text

Many cases had been studied for the first mode vibration and for static deflection, where the nature and position of the applied load were changed, and the number of collocated piezoelectric was varied. Fig.7 to Fig.10 show the results of the software simulations for these different cases.

The applied load was about 10 N and its position changed, where applied first at a = l/2 and then applied at a = l, and the piezoelectric collocated pairs number was changed to be single piezoelectric collocated pair at $x = l/2$, to be double piezoelectric collocated pairs at $x_1 = l/4$ and $x_2 = 3l/4$, and finally to be triple piezoelectric collocated pairs at $x_1 = l/4$, $x_2 = l/2$, and $x_3 = 3l/4$.

In all above cases the piezoelectric collocated pairs exhibit a significant ability to reduce the smart beam deflection in compare with the ordinary beam deflection, in Table 2 and Table 3 the percentage of the smart beam deflection reduction relative to the ordinary beam deflection had been summarized

The simulation of the smart beam without voltage amplifier and controller was didn't exhibits any reduction in beam deflection and this was expected because of that the voltage generated by the sensor can not actuate the piezo-actuator to be strained to the required limit. Therefore a complete system was proposed to enhance the actuator response and enable it to achieved its duty

Table 1 Numerical Values

Beam Properties	
Length	550 mm
Thickness	3 mm
Width	50 mm
Density	$2.77\times10^{3}\ kg/m^{3}$
Young's Modules	$7\times10^{10}\ N/m^{2}$
PZT Properties	
Length	50 mm
Thickness	0.25 mm
Width	25 mm
Charge constant	$-210\times10^{-12}\ m/V$
Young's Modules	$6.3\times10^{10}\ N/m^{2}$
Capacitance	$115\ nF$

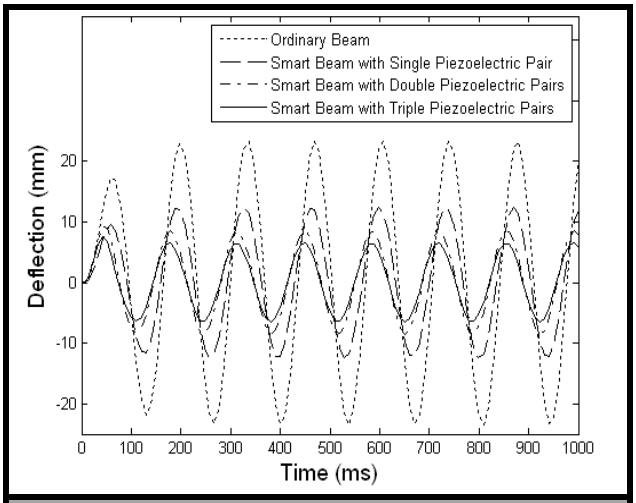

Fig.(7) Beams Deflections For Cyclic Load at $a = l/2$

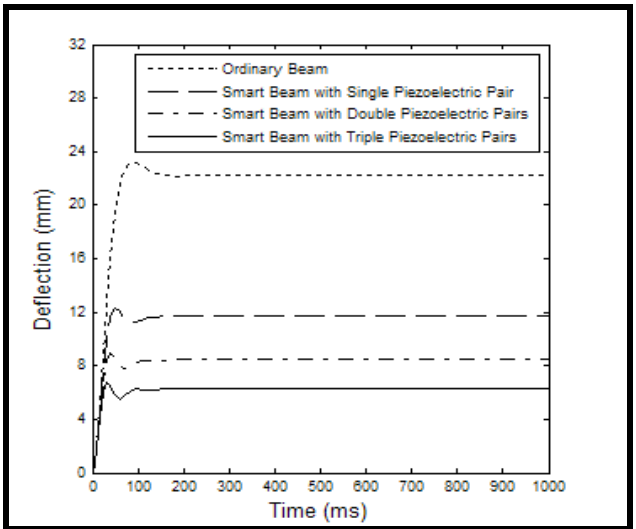

Fig.(8) Beams Deflections For Static Load at $a = l/2$

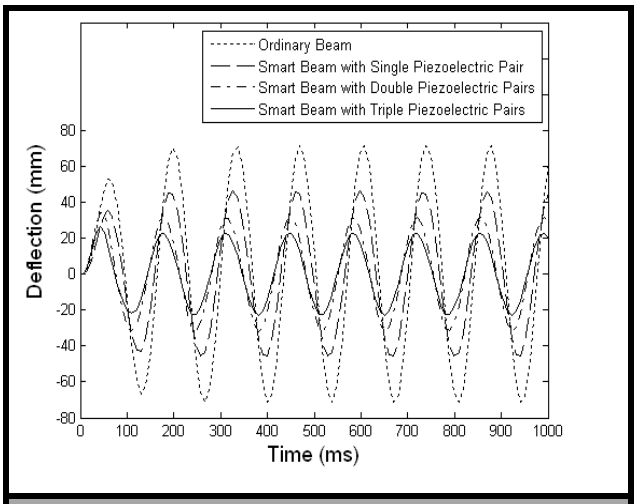

Fig.(9) Beams Deflections For Cyclic Load at $a = l$

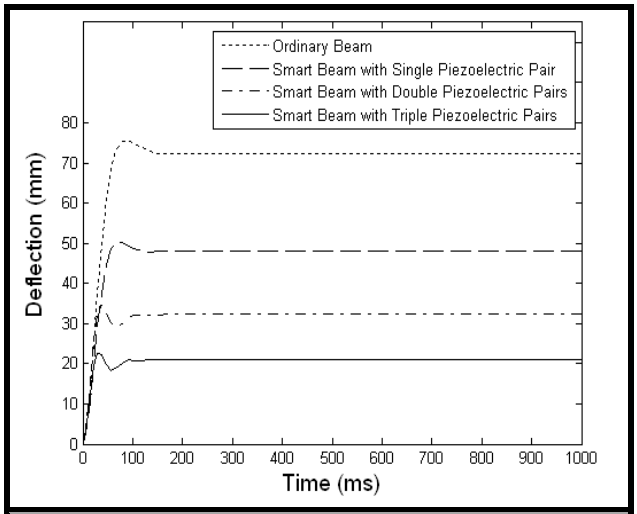

Fig.(10) Beams Deflections For Static Load at $a = l$

Table 2 The Reduction Percentage of Beam Deflection For a = l/2

Load Applied at $a = l/2$	
Cyclic Load	
No. of Piezo Pairs	**Reduction Percentage**
1	47 %
2	62 %
3	72 %
Static Load	
1	44 %
2	61 %
3	72 %

Table 3 The Reduction Percentage of Beam Deflection For a = l

Load Applied at $a = l$	
Cyclic Load	
No. of Piezo Pairs	**Reduction Percentage**
1	33 %
2	55 %
3	68 %
Static Load	
1	30 %
2	53 %
3	69 %

7. Conclusions

It has been shown that the best result of deflection reduction is obtained by increasing the number of the collocated actuator / sensor pairs for the case of multi collocated actuator / sensor pairs, but for single collocated actuator / sensor pair the best reduction is done if the collocated actuator / sensor pair is bonded exactly at the expected location of maximum deflection

The simulation of the smart beam without voltage amplifier and controller was didn't exhibits any reduction in beam deflection

8. References

[1] Aldraihem, O. J., Singh, T., and Wetherhold, R. C. (1997). Realistic determination of the optimal size and location of piezoelectric actuator/sensor. IEEE proceedings of the international conference on control applications, Piscataway, NJ (pp.435–440).

[2] Bailey, T., and Hubbard Jr., J. E. (1986). Distributed piezoelectric polymer active vibration control of a cantilever beam. Journal of Guidance, 8(5), 605–611.

[3] Belouettar S. , Azrar L., Daya E. M., Laptev V., and Potier-Ferry M. (2007). Active control of nonlinear vibration of sandwich piezoelectric beams: A simplified approach. Computers and Structures

[4] Choi, S. B., Park, Y. K., and Fukuda, T. (1998). A proof of concept, investigation on active vibration control of hybrid smart structures. Mechatronics, 8, 673–689.

[5] Clark, R. L., Saunders, W. R., and Gibbs, G. P. (1998). Adaptive structures: Dynamics and control. New York: Wiley.

[6] Crawley, E.F. , and Luis, J.D.(1987).Use of piezoelectric actuators as elements of intelligent structures. AIAA Journal, 25(10),1373–1385.

[7] De Silva C. W. (2000). Vibration: Fundamentals and Practice. Boca Raton, CRC Press LLC.

[8] Halim, D., and Moheimani, S. O. R. (2002). Experimental implementation of spatial H-Infinity control on a piezoelectric laminated beam. IEEE/ASME Transactions on Mechatronics, 7(3), 346–356.

[9] Hamdan, A.M., and Nayef, A. H.(1989).Measure of modal controllability and observability for first- and second-order linear systems. Journal of Guidance, Control and Dynamics (AIAA), 12(3), 421–428.

[10] Kermani M. R., Moallem M., and Patel R. V (2004). Parameter selection and control design for vibration suppression using piezoelectric transducers. Control Engineering Practice 12, 1005-1015.

[11] Kim, Y., and Junkins, J. L. (1991). Measure of controllability for actuator placement. Journal of Guidance, Control and Dynamics (AIAA), 14(5), 895–902.

[12] Lim, K.B. , and Gawronski, W.(1993).Actuator and sensor placement for control of Flexible structures. In C.T. Leondes (Ed.), Control and dynamic systems, Advances in theory and applications, Vol.57(pp.109–152). New York: Academic Press.

[13] Moheimani, S.O.R and Fleming J. Andrew (2006). Advances in Industrial Control. Copyright by Springer-Verlag London Limited.

[14] Moheimani, S.O.R. , and Ryall, T.(1999). Consideration on placement of piezoelectric actuators that are used in structural vibration control. IEEE proceedings of the conference on decision and control, Phoenix, AZ (pp.1118–11 23).

[15] Moore, B.C.(1981).Principal component analysis in linear systems: Controllability, observability and model reduction. IEEE Transactions on Automatic Control, 26(1), 17–32.

[16] Moses, R.W. (1997).Vertical tail-buffeting alleviation using piezoelectric actuators—Some results of buffet-affected tails (ACROBAT) program. Proceedings of SPIE, Vol.3044 (pp.87–98).San Diego, CA, USA.

[17] Ogata K. (2002). Modern Control Engineering. Fourth Edition, published by Prentice Hall, Inc.

[18] Patnaik, B., Heppler, G. R., and Wang, D. (1992). Stability analysis of a piezoelectric vibration controller for an Euler–Bernoulli beam. American control conference, San Francisco, CA.

[19] Smits, J.B. , and Choi, W.(1991).The constituent equations of piezoelectric heterogeneous Bimorphs. IEEE Transactions on Ultrasonics, Ferroelectrics and Frequency Control, 38(3), 256–270.

[20] Sun, D., and Mills, J. K. (1999a). Application of smart material actuators for control of a single-link flexible manipulator. International federation of automatic control (IFAC) world congress, Beijing, China.

[21] Sun, D., and Mills, J. K. (1999b). Study on piezoelectric actuators in control of a single-link flexible manipulator. IEEE international conference on robotics and automation, Vol.2 (pp.849–854).Detroit, Michigan, USA.

[22] Vasques C. M. A. and Dias Rodrigues (2006). Active vibration control of smart piezoelectric beam: J Comparison of classical and optimal feedback control strategies. Computers and Structures 84, 1402-1414.

[23] Wang, Q.M. , and Cross, L.E. (1999).Constitutive equations of symmetrical triple layer piezoelectric benders. IEEE Transactions on Ultrasonics, Ferroelectrics and Frequency Control, 46(6), 1343–1351.

[24] Yaghoobi, H., and Abed, E. H. (1999). Optimal actuator and sensor placement for modal and stability monitoring. IEEE proceedings of the American control conferences, San Diego, LA, pp.3702–3707.

[25] Yong, L., Onoda, J., and Minesugi, K. (2002). Simultaneous optimization of piezoelectric actuator placement and feedback for vibration suppression. Acta Austronautica, 50(6), 335–341.

[26] Zhang W., Meng G., Li H. (2006). Adaptive vibration control of micro-cantilever beam with piezoelectric actuator in MEMS. J Advance Manufacturing Technology, 321-327.

Nomenclature

(SI units are used, unless otherwise stated)

A	**The location of the applied load**
A_b	**The beam cross-sectional area**
$C_1, and\ C_2$	**The controller capacitances**
C_p	**The piezoelectric constant**
d_{31}	**The piezoelectric charge constant**
e_{ai}	**The exposed voltage to the *i*th actuator**
E_b	**The beam Young's modules**
E_p	**The piezoelectric Young's modules**
e_{si}	**The voltage induced by the *i*th sensor**
f	**The applied external force**
I_b	**The beam second moment of area**
$\bar{k}$	**A piezoelectric constant**
K_a	**The high voltage amplifier gain**
K_c	**The controller gain**
l_b	**The beam length**
l_p	**The piezoelectric length**
m	**The total number of the collocated piezoelectric actuator / sensor pairs**
M_{pi}	**The piezoelectric actuator control moment generated by the *i*th actuator**
M	**The applied external moment**
N	**The controlled vibration mode number**
Q	**The external shear force**
$R_1, R_2,$ $R_3\ and\ R_4$	**The controller resistances**
T	**The controller time constant**
t_b	**The beam thickness**
t_p	**The piezoelectric thickness**
$u(x)$	**The unit step function**
v	**The beam deflection**
w_p	**The piezoelectric width**
w_b	**The beam width**
x_{1i}	**The location of the closer edge of the *i*th piezoelectric**
x_{2i}	**The location of the further edge of the *i*th piezoelectric**
x_i	**The location of the center of the *i*th piezoelectric**
$Y_k(x)$	**The normalized mode shapes**
α	**The controller constant**
α_j	**A predefined constant for *j* mode**
β_j	**A predefined constant for *j* mode**
ε_{si}	**The mechanical strain of the *i*th piezoelectric sensor**
ψ_{ji}	**Piezoelectric constant for *i*th piezoelectric and for *j*th mode**
γ	**A beam constant**
ω_j	**The *j*th natural frequency**
ρ_b	**The beam density**
ρ_p	**The piezoelectric density**
ζ	**The beam damping ratio**

الخلاصة

في هذا البحث، لقد تم اشتقاق المعادلة العامة التي تصف الانحراف في العتبات النحيفة الذكية بنفس خطوات اشتقاق معادلة برنولي – اويلر مع بعض المعالجات والاضافات الرياضية لكي تنطبق على العتبات الذكية. إن وسائل هندسة السيطرة قد استخدمت لحل المعادلة التفاضلية المقترحة لحالة العتبة المثبتة من جانب واحد ، حيث مع بعض المعادلات المساعدة وبعد عدة اجراءات رياضية تم الحصول على مخطط صندوقي لاي نوع من الحمل المسلط (ثابت او دوري) كمدخل و انحراف العتبة كمخرج. ولضمان الحصول على افضل نسبة من تقليص انحراف العتبة تم اقتراح منظومة متكاملة اضافة الى العتبة الذكية تتكون من مضخم فولطية و مسيطر الكتروني. لقد تمت دراسة عدة حالات منها تغير طبيعة الحمل وعدد ازواج المحفز – متحسس وفي كل الحالات تم الحصول على نسب تقليص جيدة.

This document was created with Win2PDF available at http://www.daneprairie.com.
The unregistered version of Win2PDF is for evaluation or non-commercial use only.